

# Experimental Study on Shear Strength of Cohesive Soils Reinforced with Stone Columns

Majid Aslani · Javad Nazariafshar · Navid Ganjian

Received: 1 August 2018 / Accepted: 12 November 2018 / Published online: 15 November 2018  
© Springer Nature Switzerland AG 2018

**Abstract** Stone columns are mostly designed to carry compressive loads. However, in some cases, the movement of soil mass can result in lateral deformations, and consequently shear stresses in soil and stone column. The study presented herein is an experimental program, aimed to investigate the shear strength of soft clay bed reinforced with stone column. Modeling of undrained, short-term behavior of clay bed reinforced with stone column was performed using a large direct shear testing device with in-plane dimensions of  $305 \times 305$  mm. In this study, the effect of key parameters including area replacement ratio, stone column arrangement, normal pressures value, and stone column material was experimentally evaluated. For this purpose, three different replacement ratios, stone column arrangements (single, square and triangular) and normal pressures (35, 55 and 75 kPa) and two different materials including crushed gravel and fine-grained sand were used in experiments. Results showed that in the presence of stone column, the shear

strength and the overall stiffness of soft clay bed increased. The stone column arrangement, area replacement ratio and stone column material were also shown to have an impact on improving the shear strength. The most and the least increase in shear strength and stiffness values were related to square arrangement of columns and single column, respectively. In this study, the variation of stress concentration ratio of stone columns under shear loads were measured using suitable instruments. Also, the equivalent shear strength and equivalent shear parameters measured from experiments were compared with those predicted by analytical relationships at stress concentration value of 1 and stress concentration value obtained from experiments.

**Keywords** Stone column · Stress concentration ratio · Equivalent shear strength · Stone column arrangement · Direct shear test

---

M. Aslani · N. Ganjian  
Department of Civil Engineering, Science and Research  
Branch, Islamic Azad University, Tehran, Iran  
e-mail: aslanima59@yahoo.com

N. Ganjian  
e-mail: n.ganjian@srbiau.ac.ir

J. Nazariafshar (✉)  
Department of Civil Engineering, Shahr-e-Qods Branch,  
Islamic Azad University, Tehran, Iran  
e-mail: j.nazariafshar@qodsiau.ac.ir

## 1 Introduction

Using stone column is considered as an appropriate method for soil improvement and has proved its capability in fulfilling goals such as increasing slope stability, bearing capacity, and shear strength in silty and clayey soils, and reducing consolidation by accelerating drainage. Stone column method is employed to improve a wide range of clayey soils

used in constructing roads, embankments, reservoir foundations (Greenwood 1970; Murugesan and Rajagopal 2010). Stone columns are generally designed to carry vertical loads. However, in cases of cohesive ground or loose non-cohesive ground, lateral flow (Barksdale and Bachus 1983) might occur in soil and result in lateral thrust in stone column. Lateral flow reduces the lateral pressure of surrounding soil on stone column, and causes bulging in the column at surface levels. Lateral flow of the foundation soil leads to shear failure of the columns. Several numerical (Yoo 2010; Zahmatkesh and Choobbasti 2010; Yu et al. 2016; Murugesan and Rajagopal (2006)) and experimental (McKelvey et al. 2004; Fattah et al. 2010, 2017; Vekli et al. 2012; Ghazavi and Nazari Afshar 2013; Hasan and Samadhiya 2016; Nazariafshar et al. 2017; Miranda et al. 2017) studies have been performed to investigate the vertical bearing capacity of stone columns. Results have shown that the most important factors influencing the bearing capacity of stone columns are area replacement ratio, type of soil surrounding column, friction angle of stone material and column length. However, limited research has been performed to investigate the shear strength of ground improved with stone column.

Several techniques are used to numerically model and evaluate stone columns. These techniques include: (1) 3-dimensional modeling of stone columns, (2) modeling stone columns with an equivalent trench, (3) modeling stone column and the surrounding soil using homogenization method (equivalent area). These methods are used to calculate bearing capacity, slope stability and reduce the settlement of grounds improved with stone columns. Several studies have been performed to evaluate the amount of increase in the bearing capacity value due to the presence of stone columns, using triaxial testing device. In Triaxial tests, the goal is to model a stone columns and its surrounding soil as a unit cell.

Najjar et al. (2010) and Sivakumar et al. (2004) used triaxial device to experimentally investigate the increase of bearing capacity of soft clay due to the installation of sand column in the middle of the specimen. Tests were performed on specimens with different diameters and heights. Results showed that the strength of specimen increased with the increase of diameter and length of stone columns. Gniel and Bouazza (2008) used Triaxial tests to model reinforced stone columns and evaluate the effect of key

parameters such as reinforcing length and reinforcing materials in increasing shear strength. Results showed an increase of specimen stiffness and strength and reduced lateral expansion.

Although stress concentration ratio is an important parameter in calculations, it is not possible to be calculated in triaxial tests. One of the other methods of determining the amount of shear strength increase by stone column installation is using direct shear device. The influencing parameters on shear strength are stone columns arrangement pattern, stone material, area replacement ratio, and stress concentration ratio, and by direct shear device, the effect of the variation of such parameters on the variation of shear strength can be evaluated. Limited direct research has been performed to evaluate the shear strength of grounds reinforced with stone columns.

Murugesan and Rajagopal (2008) performed a series of plane strain experimental tests to evaluate the behavior of non-reinforced and reinforced stone columns under shear loading, and reported that shear strength value increased due to the presence of non-reinforced and reinforced stone columns. Mohapatra et al. (2016) performed several direct shear tests are performed on granular columns with and without encasement in a shear box. Tests are conducted at different normal pressures. Two different diameters of columns, three types of encasements and three different plan configurations are studied in this research work. Increase in shear strength was observed with an increase in area replacement ratio.

Results from the performed studies showed that the analytical analyses were carried out to determine the safety factor of the stability of slopes placed on stone column-reinforced beds. In several studies the modeling was performed by converting the 3-Dimensional arrangement of stone columns to an equivalent trench and equivalent area (Christoulas et al. 1997; Abush-arar and Han 2011; Zhang et al. 2014; Ng and Tan 2015; Chen et al. 2015; Das and Deb 2017).

Most of the research on the shear strength of stone column-reinforced grounds has been carried out using numerical methods, and limited experimental investigations, mostly with low stone column area replacement ratios, have been performed and there is a lack of laboratory research in this area. Accordingly, in this study, the shear strength of very soft soil reinforced with ordinary stone column was experimentally investigated using direct shear device. The impact of

different parameters including stone column arrangement pattern, area replacement ratio, stress concentration ratio and stone material on shear strength was investigated under different normal stresses. Stress concentration ratio is important in predicting the beneficial effects of stone column reinforced ground especially in the settlement and stability analysis. This study was the first study to record the variation of stress concentration ratio during the experiment using a special instrument installed on top of the specimen. The value of stress concentration ratio has not been calculated in laboratory studies and under shear loads and it was considered to be the conservative value of 1. One of the other goals of this research is to evaluate and compare the equivalent shear strength parameters obtained from experiments against those obtained from the typical analytical relationships available in the literature. According to the results, it is clear that in all cases the experimental shear strength parameters are higher than those obtained from the analytical relationships in which the effect of stress concentration ratio is not considered. Using these relationships is therefore conservative, and it is required that the accurate value of stress concentration ratio be calculated and used in the relationships.

## 2 Materials and Methods

This study aims to investigate the shear strength of soft cohesive soils reinforced with stone column. A large direct shear box having plan size of 305 × 305 mm and a depth of 152.4 mm was used for physical modeling and applying shear loading. When the bottom box of direct shear device is displaced horizontally, shear loads are applied on the stone column, and this state simulates the behavior of stone column under the movement of surrounding soil mass. As the dimension of the test set-up are fairly small compared with typical dimensions of full-scale granular columns, it is reported in the literature that direct shear tests should be performed considering the normal stress level on the real stone column in the field. This would avoid discrepancy between the observed behavior of columns with prototype dimensions and columns with model scale dimensions (Murugesan and Rajagopal 2008; Mohapatra et al. 2016).

## 3 Material Properties

### 3.1 Clay and Stone Materials

In this study, clayey material were prepared using a locally available soil and crushed gravel and fine-grained sand were used as the stone column materials. Table 1 represents clayey soil properties in experimental tests. As the aim of this study was to evaluate the shear strength of soft soils reinforced with stone columns, a cohesive soil with cohesion value lower than 12 kPa was selected as the bed material. To define the water content value corresponding to the desired cohesion, a series of small direct shear tests were carried out on specimens with in-plane dimensions of 50 × 50 mm and height of 25 mm, under different water contents. Shear strength parameters of  $c = 11$  kPa and  $\phi = 1^\circ$  were obtained at the water content value of 29.2%.

Fine-grained sand with particle size ranging from 0.425 to 1.18 mm and with ( $D_{10}$ ) and ( $D_{50}$ ) of (0.43) and (0.52), respectively, and crushed gravel with particle size ranging from 2 to 8 mm and with  $D_{10}$  and  $D_{50}$  of 2.2 and 4.2, respectively, were used as the stone column materials. Large direct shear tests were performed to determine the shear strength parameters of stone column materials. Properties of fine-grained sand and crushed gravel are presented in Tables 2 and 3, respectively. The gradation curve of stone column materials and clayey soil are illustrated in Fig. 1. The diameters of the model stone columns were smaller than those in the field. Thus, to simulate the real

**Table 1** Properties of clay

Parameters	Value
Specific gravity	2.7
Liquid limit (%)	44
Plastic limit (%)	20
Plasticity index (%)	24
Optimum moisture content (%)	19.5
Maximum dry unit weight	20.3 kN/m <sup>3</sup>
Minimum dry unit weight	17 kN/m <sup>3</sup>
Bulk unit weight at 29.2% water content	18 kN/m <sup>3</sup>
Cohesion	11 kPa
Friction angle	1°
Unified system classification (USCS)	CL

**Table 2** Properties of stone column material (S)

Parameters value	Value
Specific gravity	2.66
Maximum dry unit weight	17.5 3 kN/m <sup>3</sup>
Minimum dry unit weight	15.4 3 kN/m <sup>3</sup>
Bulk unit weight for test at 56% relative density	16.5 3 kN/m <sup>3</sup>
Internal friction angle ( $\phi$ ) at 56% relative density at 30.5 mm displacement	31
Uniformity coefficient (Cu)	1.28
Curvature coefficient (Cc)	0.93
Unified system classification (USCS)	SP

**Table 3** Properties of stone column material (G)

Parameters	Value
Specific gravity	2.7
Maximum dry unit weight	17 kN/m <sup>3</sup>
Minimum dry unit weight	14.7 kN/m <sup>3</sup>
Bulk unit weight for test at 80% relative density	16.5 kN/m <sup>3</sup>
Internal friction angle ( $\phi$ ) at 80% relative density at 30.5 mm displacement	35
Uniformity coefficient (Cu)	2.18
Curvature coefficient (Cc)	0.85
Unified system classification (USCS)	GP

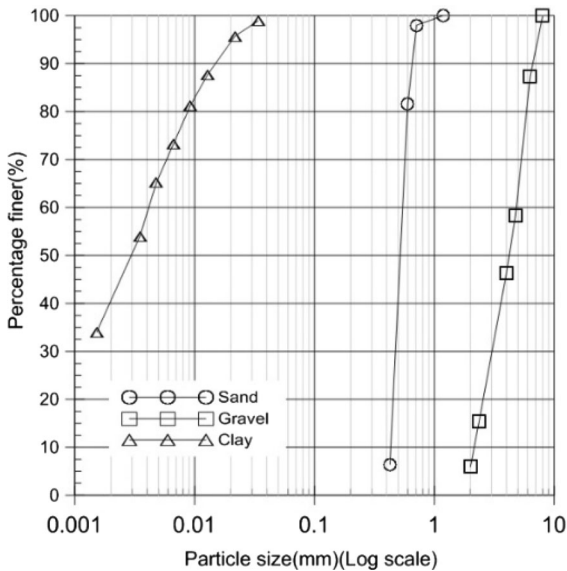


**Fig. 1** Particle size distribution for stone column and clay materials

behavior of stone columns, it was required that the particle dimensions be reduced by an appropriate scale factor to be used the models. For this purpose, the following instructions were considered in choosing the particle size of gravel and sand.

1. In practice, stone columns are constructed in typical diameters (D) varying between 0.6 m in case of stiff clays to 1.1 m in very soft clays (Ranjan 1989). Well graded stones aggregates of size (k) 2–75 mm are used, so that the ratio D/k lies typically in the range of 8 and 550. In the present study, the dimensions are reduced by an appropriate scale factor to simulate the behavior of stone columns installed in the field (Hasan and Samadhiya 2016; IS: 15284 (part 1) 2003).
2. Studies by Fox (2011) and Stoeber (2012) show that the maximum diameter of stone particle should be  $\frac{1}{10}$  of the diameter of column.
3. According to ASTM-D-4767, for triaxial test specimens the ratio between diameter of stone particle and diameter of the tested sample should be  $\frac{1}{6}$ .
4. Nayak (1983) and Fattah et al. (2010) reported that ratio of column diameter to stone particle diameter should be between  $\frac{1}{6}$  and  $\frac{1}{7}$ .
5. Another issue that should be considered in the experiments is the maximum and minimum stone particle diameter that can be tested in direct shear device. According to ASTM D-3080 standard, the maximum particle diameter should not exceed the

longitudinal dimensions of the device or  $\frac{1}{6}$  of the inner height of shear box whichever is lower. Thus, the maximum particle size that can be used in direct shear device is 25.4 mm.

As presented in Table 4, the minimum and maximum stone column diameters are 62.5 and 169 mm, respectively. Considering the column to stone particle diameter ratio of  $\frac{1}{6}$ , maximum stone particle diameter should be between 10 and 17 mm. Accordingly, stone particles with diameters ranging from 2 to 8 mm were selected for this study.

### 4 Testing Procedure

#### 4.1 Large Direct Shear Tests (LDST)

Large direct shear box (LDST) consists of upper and lower boxes. The bottom box moves in horizontal direction on smooth rollers and the top box is fully constrained from lateral movement. The Vertical and shear forces developed are continuously recorded by an S-type load cell of 20 kN capacity. Large direct shear box having plan size of (305 × 305 mm) and a depth of 140 mm 152.4 mm. A Linear Variable Differential Transformer (LVDT) was used to measure horizontal displacement (Fig. 2). The achieved data from the experiments were collected using a data logger and all the information including data on

normal and shear forces and horizontal displacements were recorded. In this study, the soil samples were sheared at a uniform displacement rate of 1 mm/min.

One of the objectives of this study was to calculate the stress concentration ratio of stone columns in different arrangement patterns illustrated in Table 4. Stress concentration ratio is the ratio of the stress carried by stone column to that carried by the surrounding soil, and can be calculated using Eq. (1). For this purposed, the direct shear device was modified. Two miniature load cells with capacity of 5 kN were employed. The load cells were mounted on the rigid loading plate with dimensions of 305 × 305 mm<sup>2</sup> and thickness of 30 mm, as shown in Fig. 3. A distinct loading plate was needed for each test as the arrangement pattern, area replacement ratio and distance between stone columns changed in different tests. 4 different steel loading plates were used for the experiments. Two load cells were placed on each loading plate, one for measuring stress in stone column, and the other for measuring stress in the soil surrounding stone column. The loading plate illustrated in Fig. 3a was used for single and square arrangement patterns, and the loading plate illustrated in Fig. 3b was used for triangular arrangement patterns. For each arrangement pattern, one of the load cells was placed on the stone column and the other on the soil, and by measuring stress values in stone column and soil, the stress concentration ratio was calculated by Eq. (1). Installation method of

**Table 4** Summary of experimental tests

Test. no	Test arrangement	Area replacement ratio Ar (%)	Test name
1	CL	0	CL
2	Center-diameter 124.5 mm	13.3	CL-G-C-13.3%
3	Center-diameter 145 mm	17.7	CL-G-C-17.7%
4	Center-diameter 169 mm	24	CL-G-C-24%
5	Square-diameter 72.5 mm	17.7	CL-G-SQ-17.7%
6	Triangle-diameter 83.5 mm	17.7	CL-G-TR-17.7%
7	Center-diameter 124.5 mm	13.3	CL-S-C-13.3%
8	Center-diameter 145 mm	17.7	CL-S-C-17.7%
9	Center-diameter 169 mm	24	CL-S-C-24%
10	Square-diameter 62.5 mm	13.3	CL-S-SQ-13.3%
11	Square-diameter 72.5 mm	17.7	CL-S-SQ-17.7%
12	Triangle-diameter 72.5 mm	13.3	CL-S-TR-13.3%
13	Triangle-diameter 83.5 mm	17.7	CL-S-TR-17.7%
14	Gravel	100	G
15	Sand	100	S

SQ square, TR triangle, C center, CL clay, G gravel, S sand

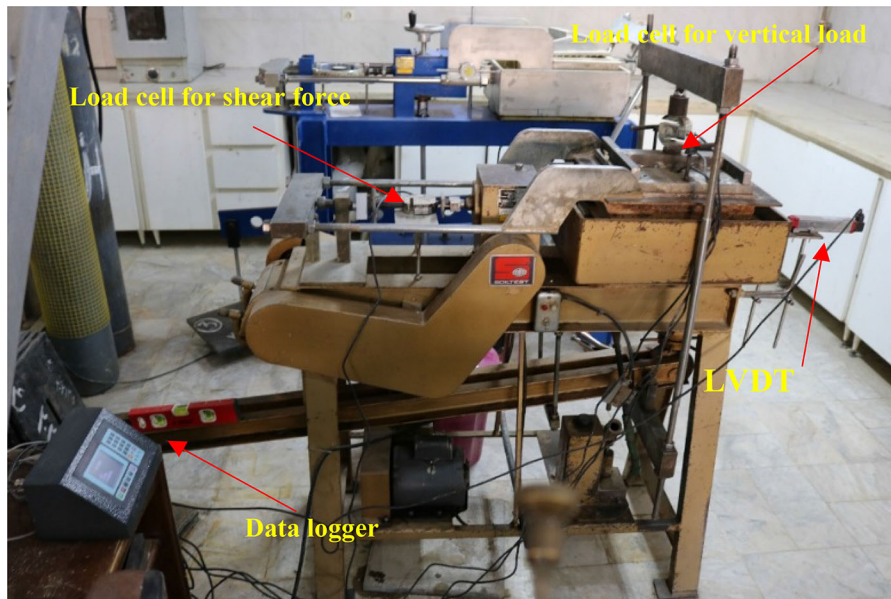


**Fig. 2** Direct shear device and installed equipment

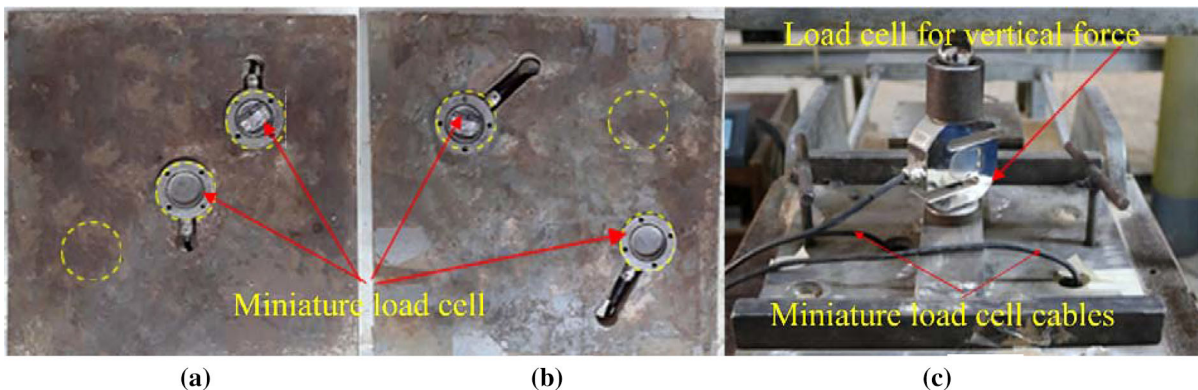


**Fig. 3** Loading plate designed for **a** single and square arrangement of stone columns, **b** triangular arrangement of stone columns, **c** installation method of S class and miniature load cells

loading plate, S class and miniature load cells illustrated in Fig. 3c.

$$n = \frac{\sigma_c}{\sigma_s} \quad (1)$$

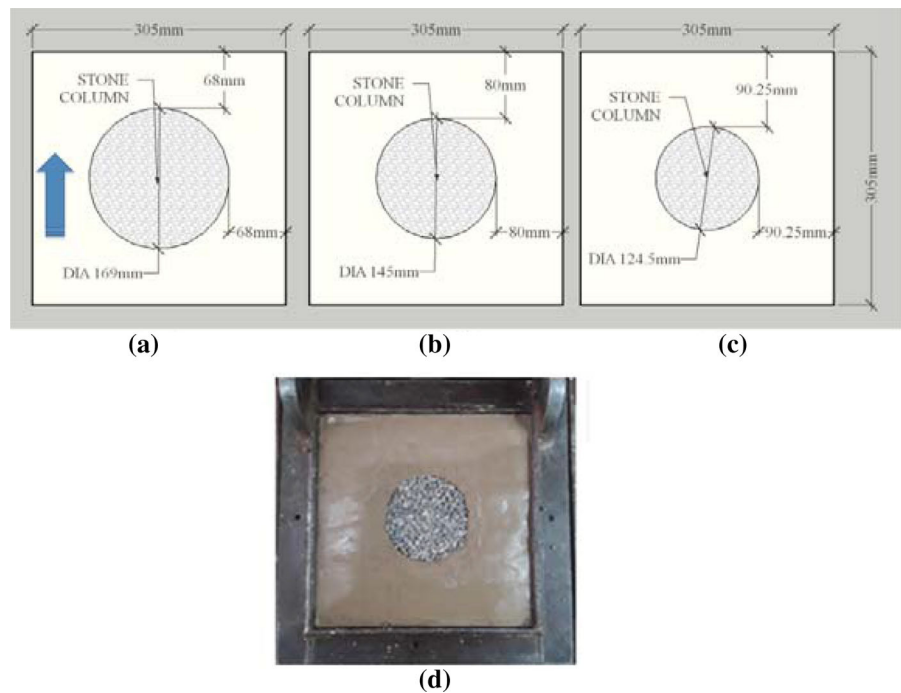
where  $n$  is stress concentration ratio,  $\sigma_c$  is stress in stone column, and  $\sigma_s$  is stress in soil.

## 5 Experimental Program

Single stone columns and group stone columns arranged in square and triangular patterns were tested

to evaluate the effect of stone column installation pattern. Experiments were performed under normal stresses of 35, 55 and 75 kPa to obtain Mohr–coulomb failure envelop. Experiments were performed at different area replacement ratios. Area replacement ratio is the ratio of column cross section area to the total device area. Table 4 summarizes the details of the tests performed in this study. Installation pattern and location of stone columns are illustrated in Figs. 4, 5 and 6. Single, square and triangular arrangements of stone columns are illustrated in Figs. 4, 5 and 6, respectively. In Table 4 the first letter of the test names represents soil bed material, the second letter

**Fig. 4** Layout of single stone columns: **a**  $Ar = 24\%$ , **b**  $Ar = 17.7\%$ , **c**  $Ar = 13.3\%$ , **d** sample in direct shear test



represents stone column material, the third letter indicates pattern of arrangement, and the last number refers to area replacement ratio. In this study, 4 series of experiments were performed to ensure the repeatability of the achieved data, and great consistency between the performed experiments. All tests were continued until the lower part of direct shear device reached a horizontal displacement of 30.5 mm. This displacement value was equal to 10% of sample length. Therefore, to eliminate boundary effects, stone columns should have a distance of at least 30.5 mm from the inner walls of the shear box.

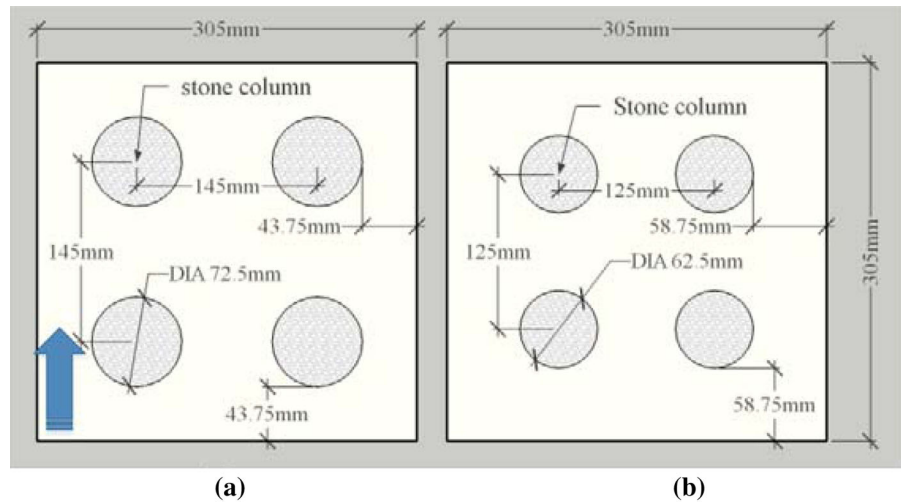
## 6 Sample Preparation

### 6.1 Preparation of Clay Bed

The clayey soil was first screened through a sieve with 1 cm aperture size to remove coarse particles and other unwanted materials. The soil was then oven-dried at 110 C for 16 h, and put in a plastic bag. The required water for the moisture content of 29.2% was added to the soil and the bag was sealed. Then, the sample was covered by nylon and left for 1 week, and in the meantime, the specimen was kneaded several

times to reach equal water content. After 7 days, water content tests were performed on samples obtained from different parts of the soil specimen to ensure water content of 29.2%. As the experiments were performed in undrained condition, a thin layer of plastic was placed at the bottom and side walls of the shear box to avoid moisture content loss during the experiments. To control the thickness of each layer, the main box wall was graded in 3 cm intervals so soft clay samples could be constructed in 3 cm layers using the unit-weight-control method. Before carrying out any tests, the main box walls were coated by a thin layer of grease to reduce any friction between the clay and the walls. To reach a unit weight of  $18 \text{ kN/m}^3$ , clay was weighed, and it was placed into the main box in the form of 3 cm layers. Figure 7a illustrates the preparing steps of the clay bed. The layers were compacted using a special hammer (150 mm  $\times$  150 mm and  $w = 2 \text{ kg}$ ). A series of steel bars with a diameter of 10 mm and a length of 10 mm were placed under the special hammer for kneading each clay layer. This helped to reduce leftover air voids in the test bed and to connect clay layers to one another. Each soil layer was compacted to reach 3 cm in height. This preparation method was repeated for all experiments. After preparing the clay bed, the surface of clay layer

**Fig. 5** Layout of stone columns with square arrangement pattern  
**a**  $Ar = 17.7\%$ ,  
**b**  $Ar = 13.3\%$ , **c** sample in direct shear test



was leveled. Throughout the course of the experiments, the water content was measured to ensure the desired percentage of water. The results showed that the water-content percentage variations were below 1% in all tests.

## 7 Stone Column Construction

In this study, all stone columns were installed by replacement method. Hollow open-ended steel pipes with outer diameter equal to that of stone columns were used to construct stone columns. The pipes had to be smooth and seamless. The selected wall thickness selected for steel pipes was 2 mm to reduce disturbance during pipe installation. For installation the inner and outer surface of steel pipe were coated by a

thin layer of oil to facilitate the movement of pipe in the soil layer and to avoid soil disturbance. The pipe was then pushed into soil layer until it reached the bottom of the shear box. The pipes were pushed into the soil and their vertical alignment was controlled using a special level during installation. After pushing the pipe into the soil layer, the soil inside the pipe was discharged using a steel spiral auger. The auger diameter was slightly smaller than the diameter of the pipe. Thereafter the soil was discharged, the pipe was pulled out slowly. The removal rate of pipe was slow enough to avoid any change in the diameters of the hole. After removing the pipe, stone column material required for the hole was weighed based on material unit weight ( $16.5 \text{ kN/m}^3$ ) and hole volume and poured into the hole, and compacted in five 3 cm-thick layers. Figure 7b illustrates stone column construction steps.



**Fig. 6** Layout of stone columns with triangular arrangement pattern  
**a**  $A_r = 17.7\%$ ,  
**b**  $A_r = 13.3\%$ , **c** sample in direct shear test

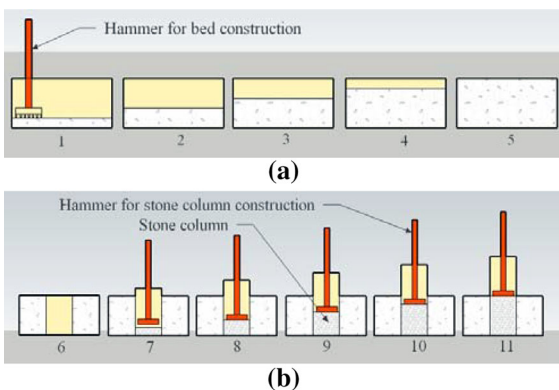
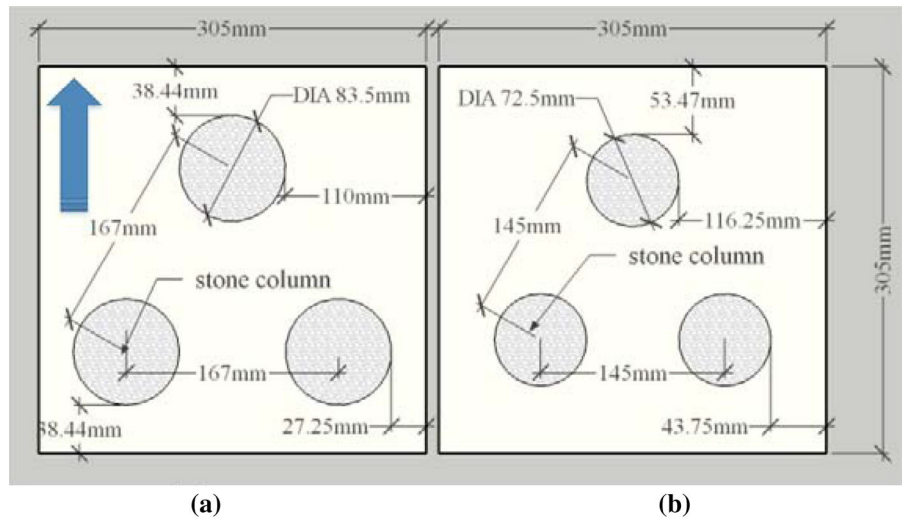


**Fig. 7** Preparing steps of samples in direct shear box **a** stage of bed construction, **b** stage of stone columns construction

Stone column material was uniformly compacted to achieve stone column with uniform unit weight. The same compaction energy of  $67 \text{ kJ/m}^3$  was used in all tests. The observations during compaction showed that this energy level provided the required unit weight without causing lateral expansion of the stone column. According to ASTM D-3080 the tamper used to compact the material should have a contact area with the soil equal to or less than  $\frac{1}{2}$  the area of the shear box. In this study, the ratio of tamper area to stone column cross-section area was equal to or less than 0.5.

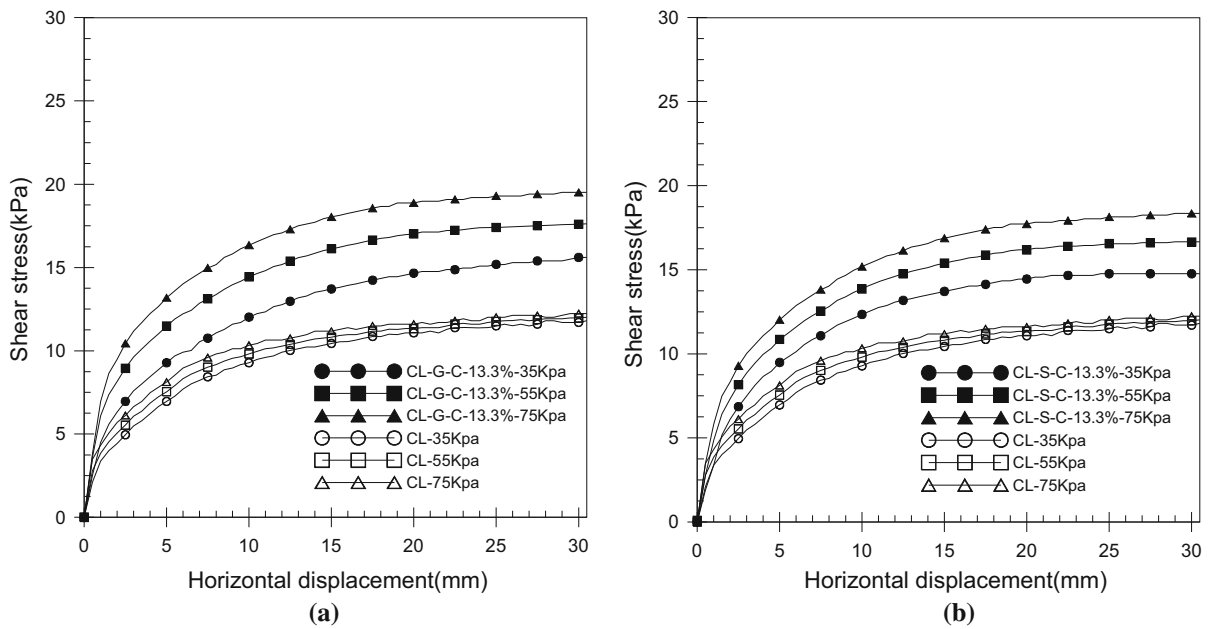


**Fig. 8** Shear stress versus horizontal displacement  $Ar = 13.3\%$ : **a** CL-G-C, **b** CL-S-C

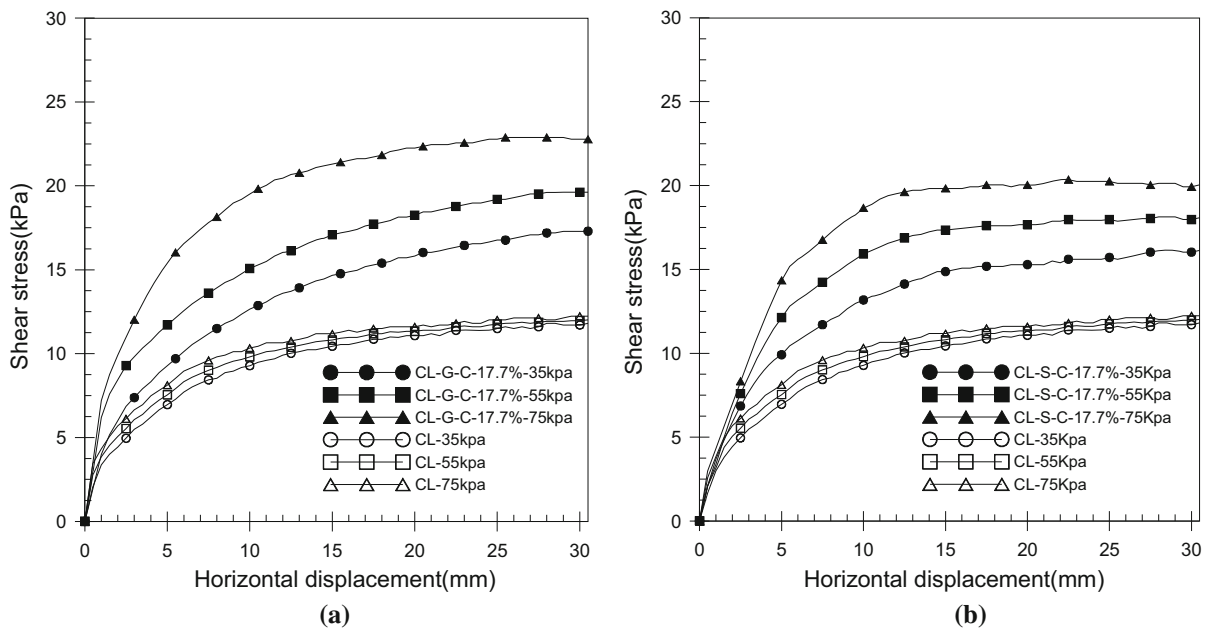


**Fig. 9** Shear stress versus horizontal displacement  $Ar = 17.7\%$ : **a** CL-G-C, **b** CL-S-C

## 8 Results and Discussion

### 8.1 Effect of Stone Columns

Figures 8, 9, 10, 11, 12 and 13 illustrate diagrams of shear stress versus horizontal displacement for

different stone column installation patterns, area replacement ratios, and stone materials (sand or gravel), under normal stress values of 35, 55 and 75 kPa. Results from Figs. 8, 9, 10, 11, 12 and 13 show that stone column installation leads to an increase in the shear strength value of soft clay bed.

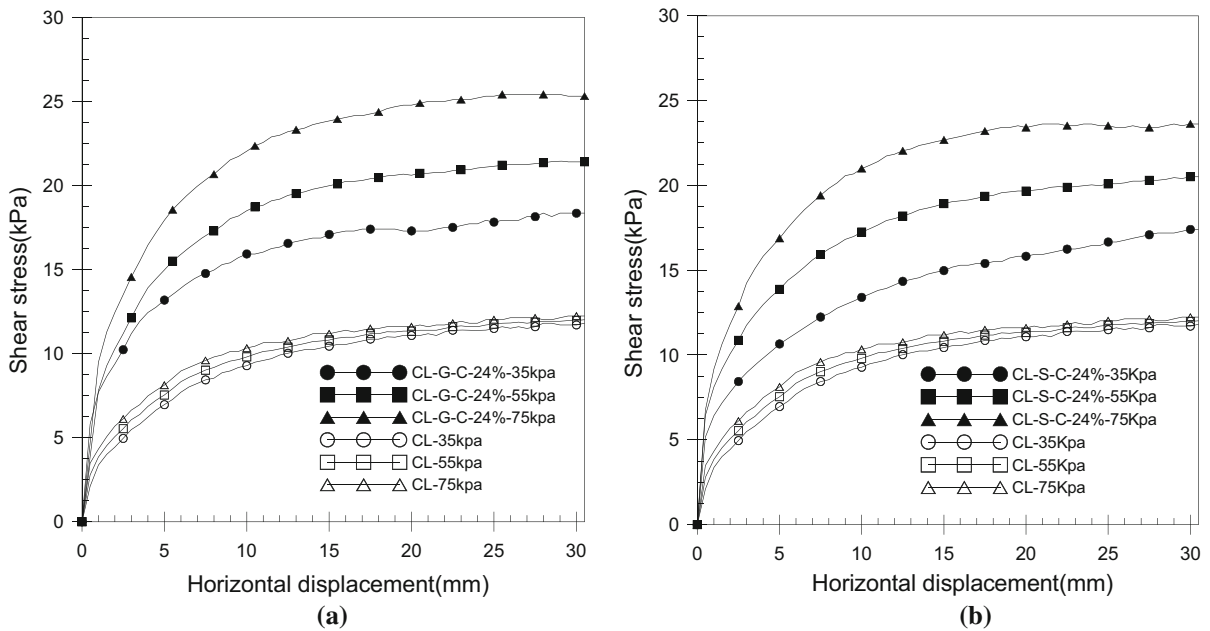


**Fig. 10** Shear stress versus horizontal displacement  $A_r = 24\%$ : **a** CL-G-C, **b** CL-S-C

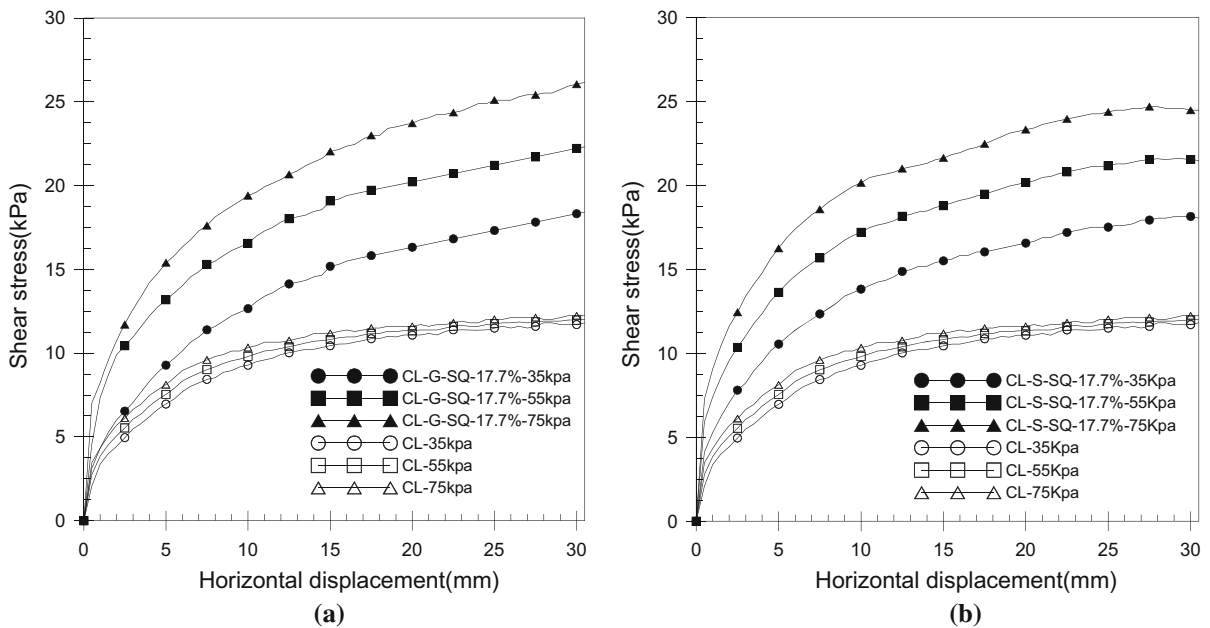


**Fig. 11** Shear stress versus horizontal displacement  $A_r = 17.7\%$ : **a** CL-G-SQ, **b** CL-S-SQ

Stone column together with soft clay bed perform as a composite material and mobilize higher shear strength compared to soft clay bed itself. With the increase of area replacement ratio, shear strength increases due to the increase of stone column area effective in shear

surface. Table 5 presents the amount of increase in the shear strength value of stone column-reinforced clay bed at 10% horizontal displacement, for different stone column installation patterns and under different normal stress values. Results from Table 5 show that

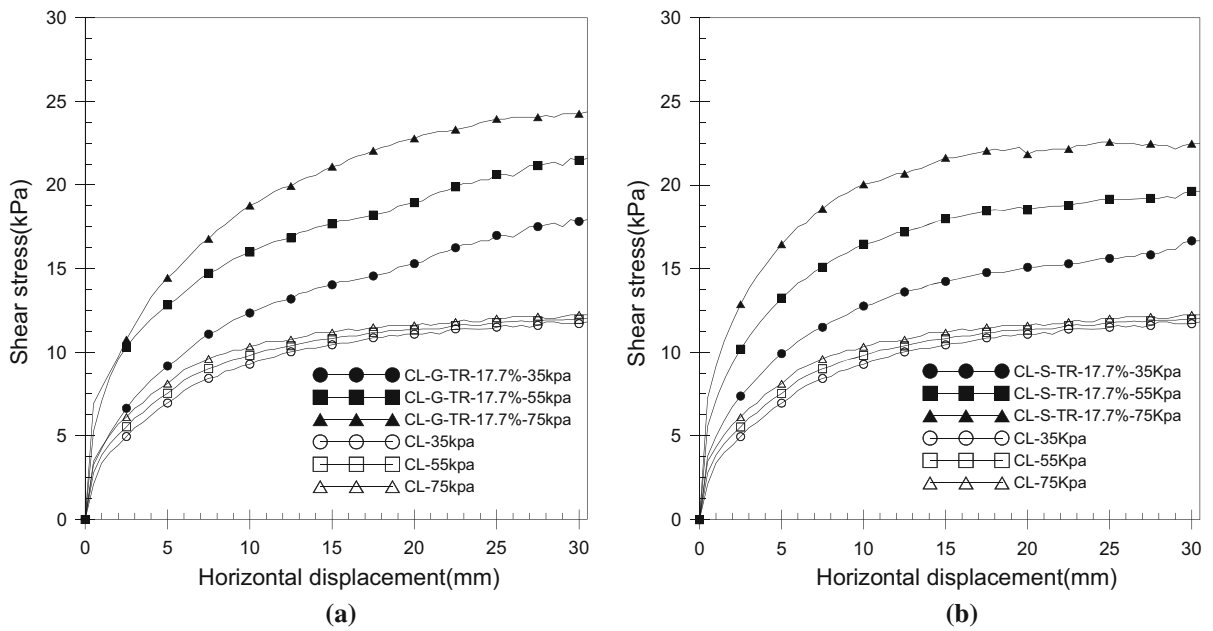


**Fig. 12** Shear stress versus horizontal displacement  $A_r = 17.7\%$ : **a** CL-G-TR, **b** CL-S-TR

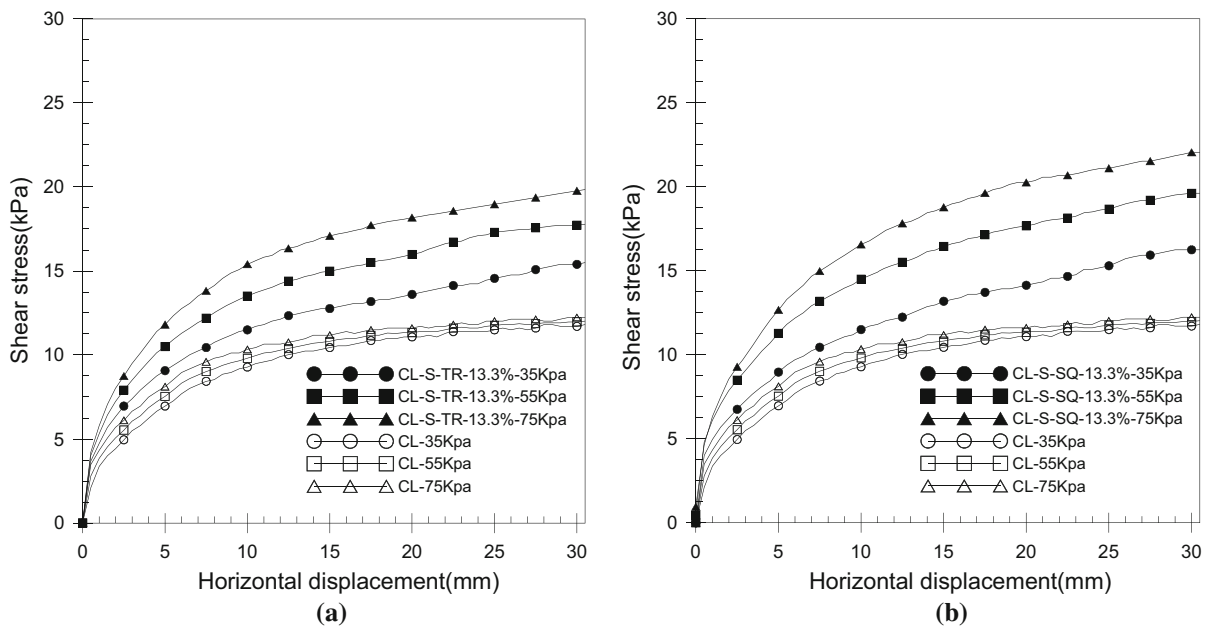


**Fig. 13** Shear stress versus horizontal displacement  $A_r = 13.3\%$ : **a** CL-S-TR, **b** CL-S-SQ

for tests with the same area replacement ratio, the amount of shear strength increase is higher for stone columns installed in square and triangular patterns in comparison to single stone columns, and the highest value is for square pattern. One of the reasons of shear strength increase in square and triangular patterns is

the increased confining pressure on the soil between stone columns. This makes the soil between stone columns mobilize higher shear strength compared to the soil surrounding single stone column. Another reason is the increase in lateral surface area of stone columns resulted from changing the arrangement from

**Table 5** Shear strength of clay bed reinforced with stone column

Test. no	Test name	Increase of shear stress (%)		
		Vertical stress		
		35 kPa	55 kPa	75 kPa
1	CL	–		
2	CL-G-C-13.3%	33	50	62
3	CL-G-C-17.7%	47	68	81
4	CL-G-C-24%	57	83	100
5	CL-G-SQ-17.7%	58	92	108
6	CL-G-TR-17.7%	50	83	92
7	CL-S-C-13.3%	25	42	46
8	CL-S-C-17.7%	33	50	62
9	CL-S-C-24%	50	75	86
10	CL-S-SQ-13.3%	42	67	69
11	CL-S-SQ-17.7%	58	83	92
12	CL-S-TR-13.3%	33	50	54
13	CL-S-TR-17.7%	42	67	77

single column to square and triangular patterns. The increase in lateral surface area improves the lateral force on stone column, and results in a higher shear strength mobilization of stone material. Results from Figs. 8, 9, 10, 11, 12 and 13 show that the amount of increase in shear strength was not significant for area replacement ratios lower than 15%. However, for area replacement ratios higher than 15% the amount of increase in shear strength was noticeable. In addition, the slope of shear stress-horizontal displacement curves increased, showing that the overall stiffness improved due to stone column installation. It can also be said that stone column installation pattern had an effective role in increasing stiffness, where the highest increase in stiffness was observed for square pattern. According to the Figs. 8, 9, 10, 11, 12 and 13, stone column material had an effective role in increasing shear strength, and columns filled with gravel mobilized higher shear strength compared to those filled with sand. However, due to the low shear strength of clay bed, full development of shear strength of stone material was not possible, and as a result, the difference between shear strength values of gravel columns and sand columns was not significant.

Figures 14, 15 and 16 illustrate variation of shear strength value with area replacement ratio for different

installation patterns and normal stresses. Figures 14, 15 and 16 refer to single, square and triangular patterns, respectively. According to Figs. 14, 15 and 16 the value of shear stress increases with increase of normal stress and area replacement ratio, and the maximum increase in shear strength corresponding to 10% horizontal displacement refers to square arrangement. Also, gravel columns mobilize higher shear strength compared to sand columns.

## 9 Shear Strength Parameters

Shear strength parameters obtained from experiments with different stone column installation patterns and different area replacement ratios are presented in Table 6. Results showed that the shear strength parameters of soil bed were improved by stone column installation. According to Table 6, for stone columns with the same area replacement ratio value, the maximum increase in friction angle refers to stone columns with square patterns and the minimum value refers to single stone columns. The friction angle corresponding to horizontal displacement of 10% increased from 1° to 10° due to stone column installation. Friction angle had an increasing trend with increase in area replacement ratio, particularly at area replacement ratios higher than 15%. However, the increased value was slight at area replacement ratios lower than 15%. Also, negligible variation was observed in cohesion value, and the value of cohesion at 10% displacement was equal to its initial value. Using gravel columns resulted in higher shear strength parameters compared to using sand columns. However, the difference between the obtained shear strength parameters was not significant due to the low cohesion of clay layer which did not allow full development of shear strength of stone column material.

## 10 Equivalent Shear Strength

In studying the bearing capacity, settlement and stability of soil bed reinforced with stone columns, the stone column and the surrounding soil can be modeled according to Fig. 17a. Although the tributary area of soil surrounding each stone column form a regular hexagon, it can be replaced with an equivalent

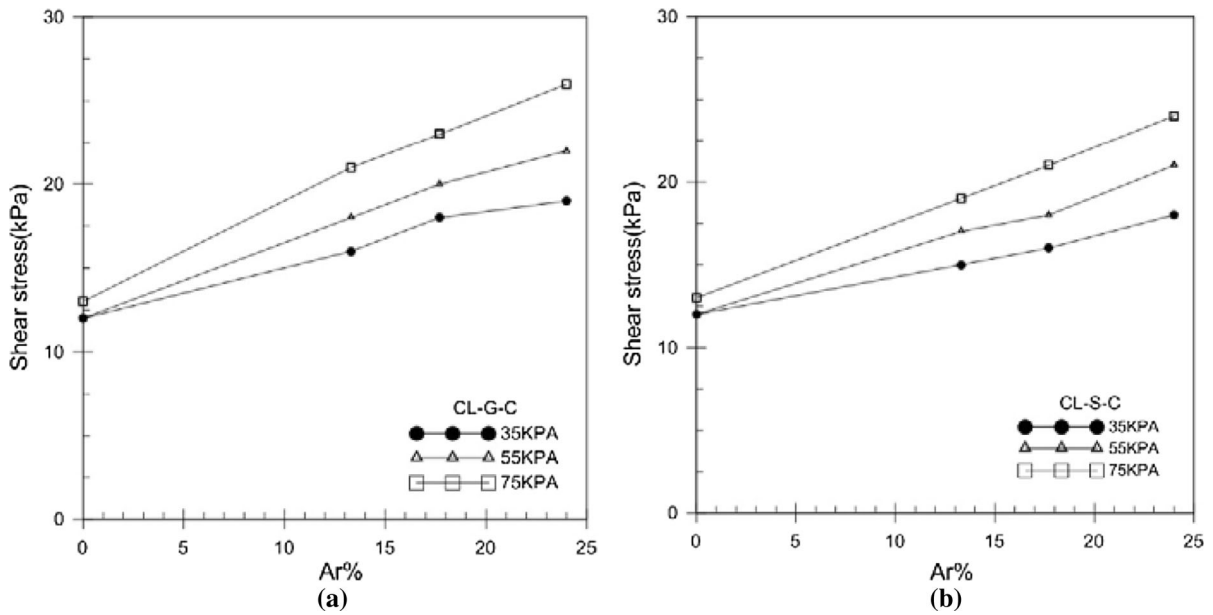


**Fig. 14** Variation of shear stress mobilized versus area replacement ratio (Ar) **a** CL-G-C, **b** CL-S-C

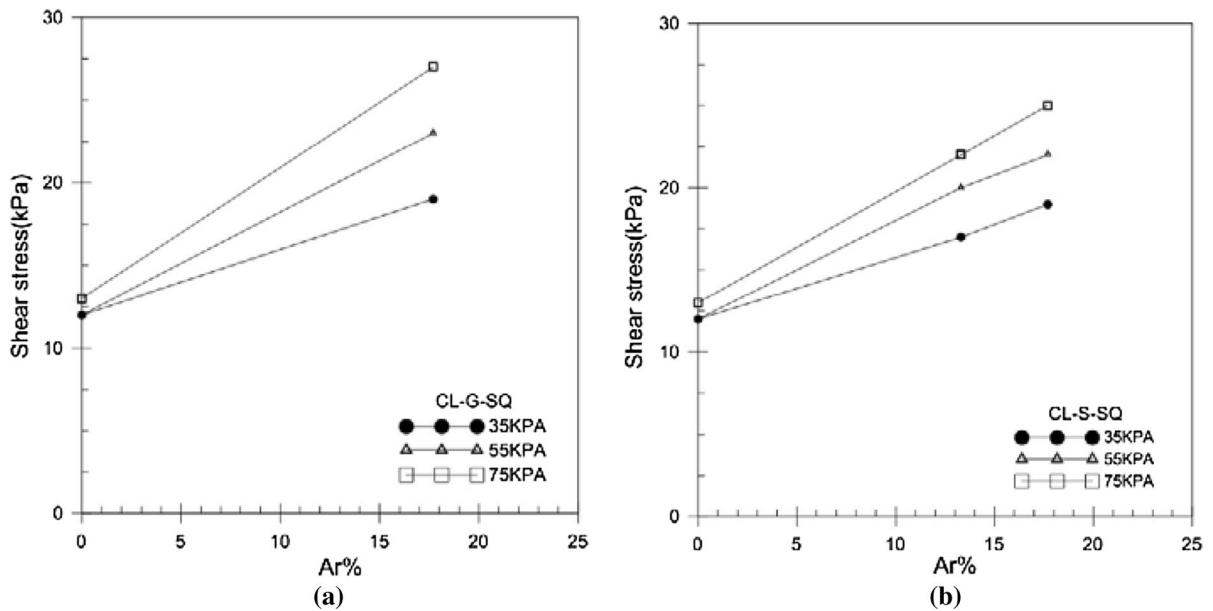


**Fig. 15** Variation of shear stress mobilized versus area replacement ratio (Ar) **a** CL-G-SQ, **b** CL-S-SQ

circle with the same area. The formed column containing the stone column and the surrounding soil is considered as a unit cell (Fig. 17b, c). However, stone column and the surrounding soil together form a heterogeneous medium. For simplification, the heterogeneous unit cell is converted to a homogenous one. For this purpose, the stone column and the surrounding

soil are replaced with an equivalent homogenous soil with improved properties. One of the methods of calculating equivalent soil parameters is to average soil and column parameters weighted by their corresponding area. This method is a common method in estimating bearing capacity, settlement and especially slope stability (Abusharar and Han 2011; Zhang et al.

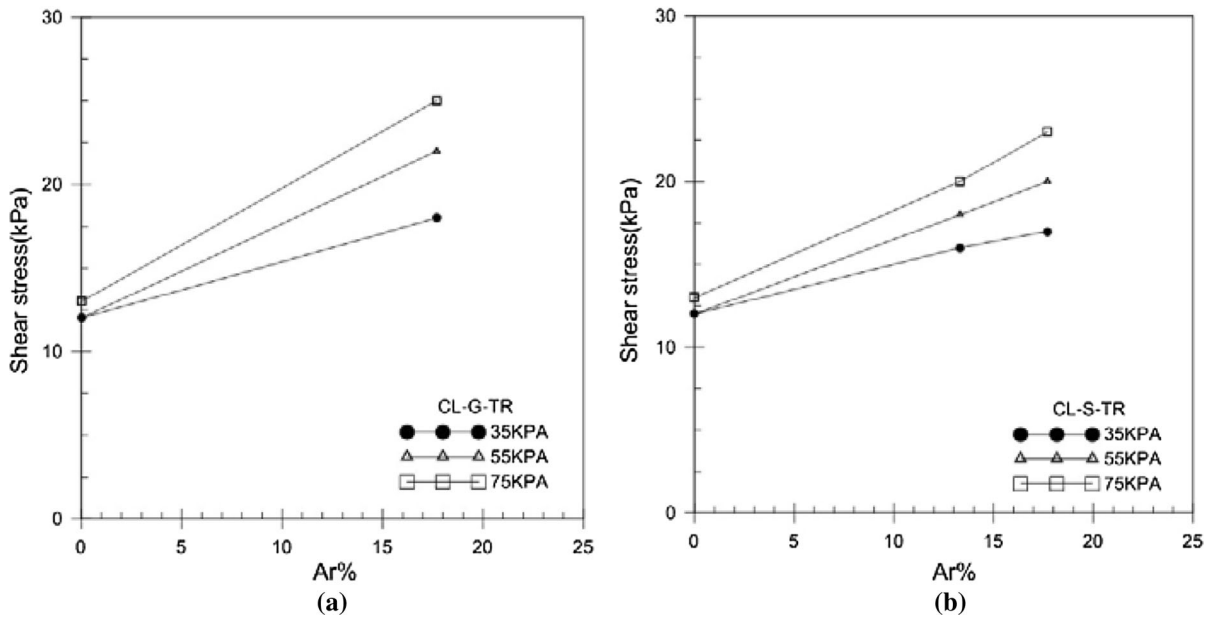


**Fig. 16** Variation of shear stress mobilized versus area replacement ratio (Ar) **a** CL-G-TR, **b** CL-S-TR

**Table 6** Shear strength parameters obtained from experiments

Test. no	Test name	Area replacement ratio Ar (%)	Cohesion (kPa)	Internal friction (°)
1	CL	0	11	1
2	CL-G-C-13.3%	13.3	12	6
3	CL-G-C-17.7%	17.7	12	8
4	CL-G-C-24%	24	12	10
5	CL-G-SQ-17.7%	17.7	13	10
6	CL-G-TR-17.7%	17.7	13	9
7	CL-S-C-13.3%	13.3	12	5
8	CL-S-C-17.7%	17.7	12	6
9	CL-S-C-24%	24	12	9
10	CL-S-SQ-13.3%	13.3	12	8
11	CL-S-SQ-17.7%	17.7	13	9
12	CL-S-TR-13.3%	13.3	12	6
13	CL-S-TR-17.7%	17.7	12	8
14	G	100	12	35
15	S	100	5	31

2014). The equivalent shear strength of unit cell can be calculated by Eq. (2).

$$\tau_{ave} = A_r \tau_c + (1 - A_r) \tau_s \tag{2}$$

where  $\tau_{ave}$  is equivalent shear strength,  $A_r$  is area replacement ratio,  $\tau_c$  is shear stress of stone column

material and  $\tau_s$  is shear stress of bed material. The weighted average of reinforced soil unit weight is calculated using Eq. (3)

$$\gamma_{ave} = A_r \gamma_c + (1 - A_r) \gamma_s \tag{3}$$

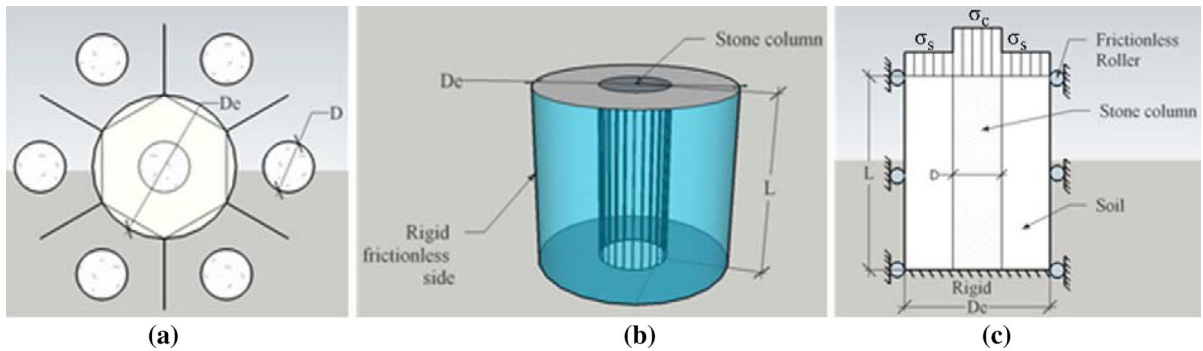


**Fig. 17** Unit cell idealization **a** plan view, **b** unit cell **c** section [7]

where  $\gamma_{ave}$  is equivalent unit weight,  $\gamma_c$  is unit weight of stone column material, and  $\gamma_s$  is unit weight of bed material.

Shear strength parameters in equivalent shear strength method are calculated using the following equations. Equation (4) is used to calculate the equivalent friction angle (Barksdale and Bachus 1983):

$$[\tan \phi]_{ave} = \frac{\gamma_c \cdot A_r \cdot \tan \phi_c + \gamma_s \cdot (1 - A_r) \cdot \tan \phi_s}{\gamma_{ave}} \quad (4)$$

where  $\phi_{ave}$  is equivalent friction angle,  $\phi_c$  is friction angle of stone column material, and  $\phi_s$  is friction angle of bed material.

Cooper and Rose (1999) proposed Eq. (5) for equivalent friction angle:

$$\phi_{ave} = \tan^{-1}(A_r \cdot \tan \phi_c + (1 - A_r) \tan \phi_s) \quad (5)$$

Cooper and Rose (1999) and Christoulas et al. (1997), proposed Eq. (6) for equivalent friction angle.

$$\phi_{ave} = A_r \phi_c + (1 - A_r) \phi_s \quad (6)$$

In Eqs. (4)–(6), the stress concentration ratio is not included, and all soil shear strength parameters are calculated by assuming that the stress concentration ratio is equal to 1.

Figures 18, 19 and 20 illustrate the failure envelope of stone column-reinforced soil at horizontal displacement of 10%, for different stone column installation patterns. Results show that shear stress increases with increase of normal stress and area replacement ratio. Also, the amount of increase in shear strength is maximum in square pattern and minimum in single pattern. Figures 18, 19 and 20 illustrate the

comparison between the equivalent shear strength values obtained from experiments and those obtained from analytical relationships. Results show that in all installation patterns, shear strength values obtained from experiments are higher than those predicted by analytical relationships.

One important point about the results is the difference between shear strength and friction angle values predicted by analytical relationships and those obtained from experiments. The difference between friction angle values predicted by Eqs. (4)–(6) and those obtained from experiments is illustrated in Table 7 for different stone column installation patterns. Results show that shear strength parameters obtained from experiments on single stone columns are in good agreement with those predicted by Eqs. (4)–(6). However, for square and triangular patterns, shear parameter values obtained from experiments are higher than those predicted by Eqs. (4)–(6). The observed difference between the results can be explained by the following reasons:

Firstly, although shear strength increases by stone column installation, the soft soil bed surrounding stone column cannot provide enough lateral pressure to mobilize shear strength of stone column material. However, analytical relationships assume that the shear strength of stone column material is fully developed. Secondly, analytical relationships do not consider stress concentration ratio, and Eqs. (4)–(6) are proposed assuming that the stress concentration ratio is equal to 1, while, in reality, the stress concentration ratio is higher than 1. In fact, calculating shear parameters based on shear strength relationships is a conservative approach, and accurate shear parameter values should be calculated by taking stress



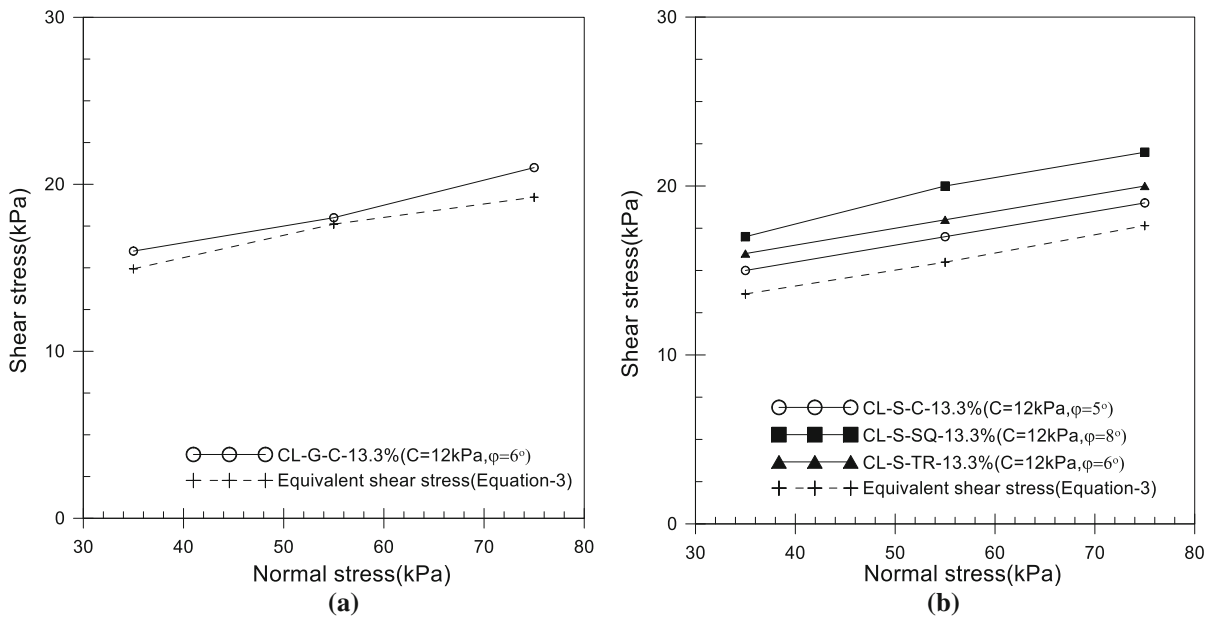


**Fig. 18** Mohr–Coulomb failure envelopes for  $A_r = 13.3\%$  and different arrangement pattern **a** gravel stone column, **b** sand stone column

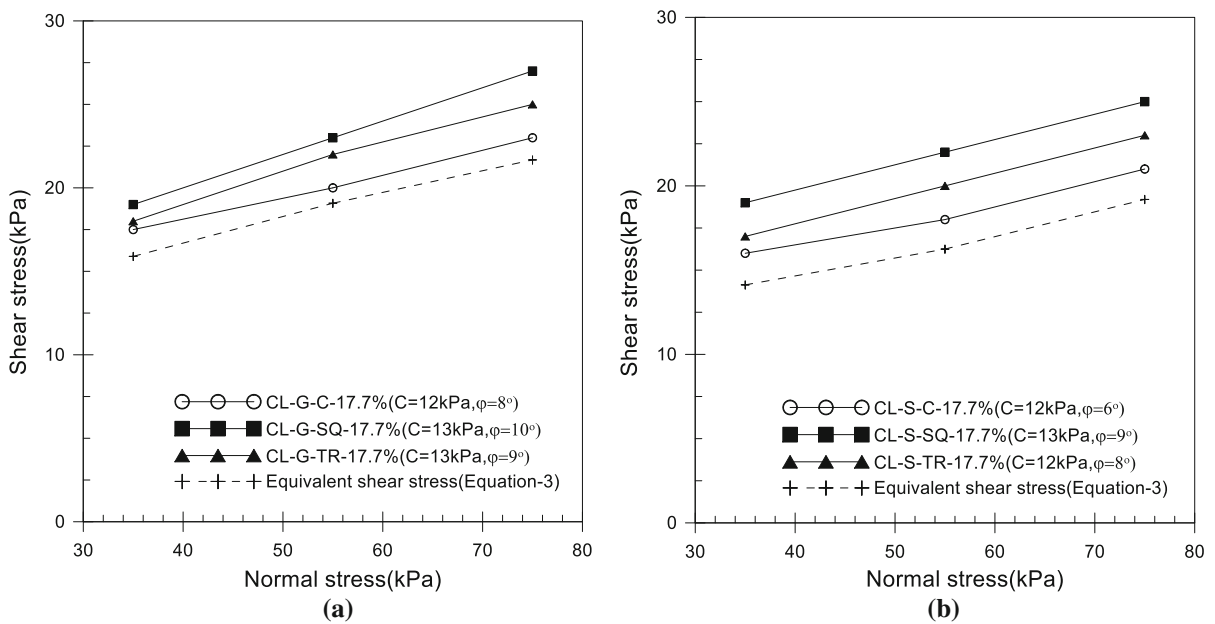


**Fig. 19** Mohr–Coulomb failure envelopes for  $A_r = 13.3\%$  and different arrangement pattern **a** gravel stone column, **b** sand stone column

concentration ratio into account. Results show that for single stone columns the stress concentration ratio is equal to 1, and for square and triangular arrangements of stone columns, stress concentration ratio is higher than 1.

### 11 Equivalent Shear Strength Calculation Considering Stress Concentration Ratio

As stated before, in this study, stress in the stone columns and the surrounding soil was measured using

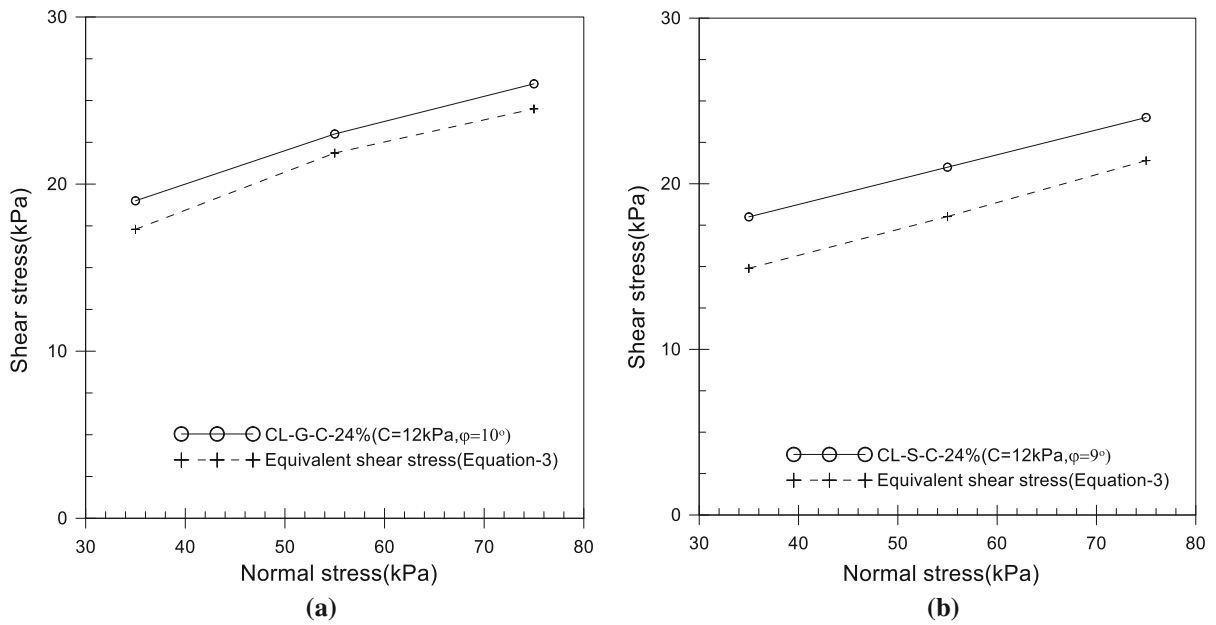


**Fig. 20** Mohr–Coulomb failure envelopes for  $Ar = 24\%$  and different arrangement pattern **a** gravel stone column, **b** sand stone column

**Table 7** Difference between friction angle values obtained from experiments and values predicted by Analytical relations

Test. no	Test name	Internal friction angle (°)			
		Test result	Eq. (4)	Eq. (5)	Eq. (6)
1	CL	1	–	–	–
2	CL-G-C-13.3%	6	6	6	5
3	CL-G-C-17.7%	8	8	8	7
4	CL-G-C-24%	10	10	10	9
5	CL-G-SQ-17.7%	10	8	8	7
6	CL-G-TR-17.7%	9	8	8	7
7	CL-S-C-13.3%	5	5	5	5
8	CL-S-C-17.7%	6	7	6	6
9	CL-S-C-24%	9	8	9	8
10	CL-S-SQ-13.3%	8	5	5	5
11	CL-S-SQ-17.7%	9	7	6	6
12	CL-S-TR-13.3%	6	5	5	5
13	CL-S-TR-17.7%	8	7	6	6
14	G	35	–	–	–
15	S	31	–	–	–

special equipment. The obtained stress values were then used in Eq. (1) to calculate stress concentration ratio. The values of stress concentration ratio corresponding to different stone column installation patterns, replacement ratios and normal stresses are illustrated in Figs. 21, 22, 23, 24, 25 and 26. Results show that the value of stress concentration ratio first

increases when the load is applied, then decreases during the experiment, and finally reaches the value of 1 at the end of the experiment (Table 8). Results also show that stress concentration ratio decreases with increase of stone column diameter.

Moreover, results show that stress concentration ratio decreases with increase of normal stress. The

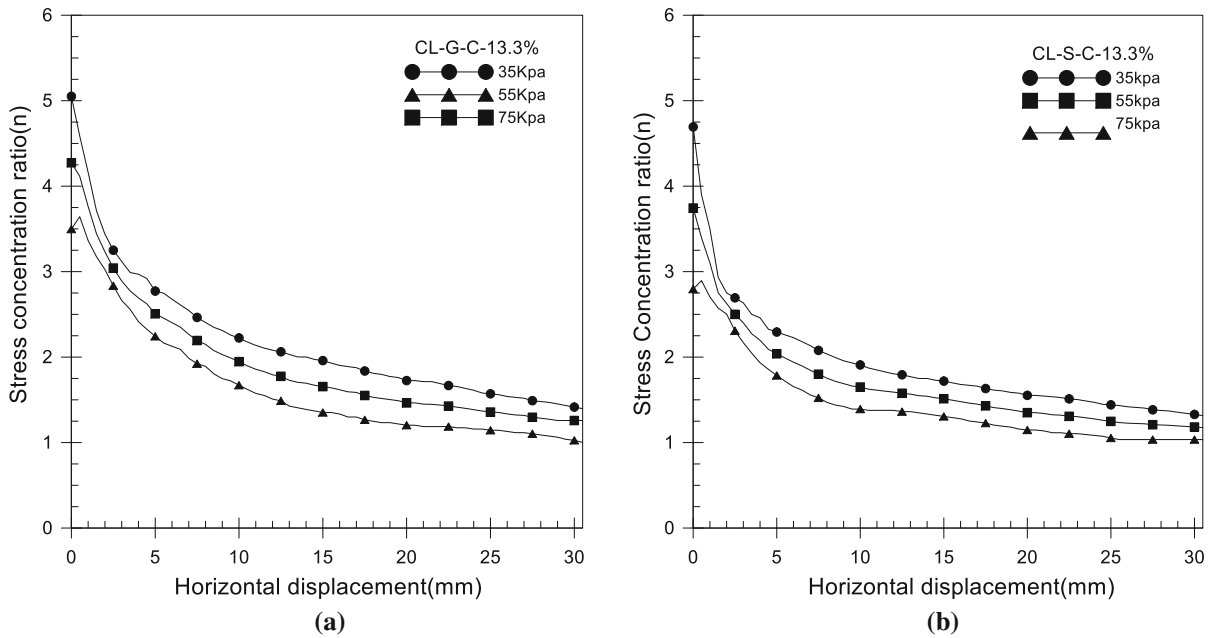


**Fig. 21** Stress concentration ratio for Ar = 13.3%: **a** CL-G-C, **b** CL-S-C

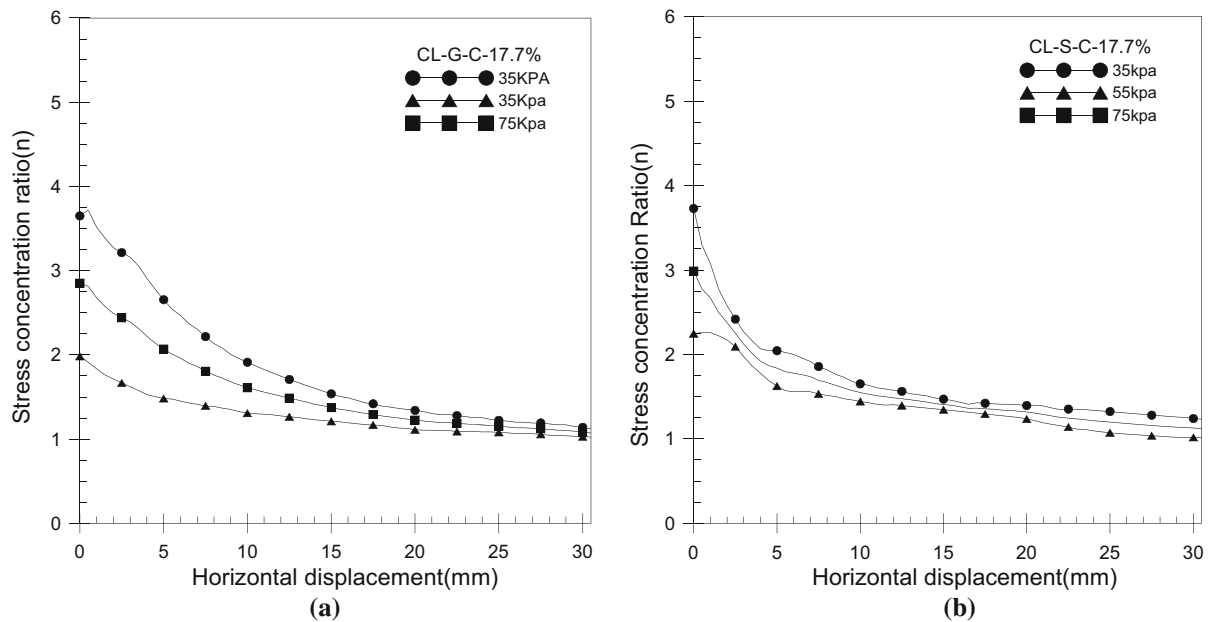


**Fig. 22** Stress concentration ratio for Ar = 17.7%: **a** CL-G-C, **b** CL-S-C

decrease in value of stress concentration ratio is due to the lack of adequate lateral confining pressure from the surrounding soft clay layer, and increasing normal stress results in bulging of stone column. Results show that the value of stress concentration ratio in square

pattern is higher than that in triangular pattern. Also, stress concentration ratio in gravel columns is higher than that in sand columns.

As previously mentioned, the effect of stress concentration ratio is not considered in Eqs. (4)–(6),

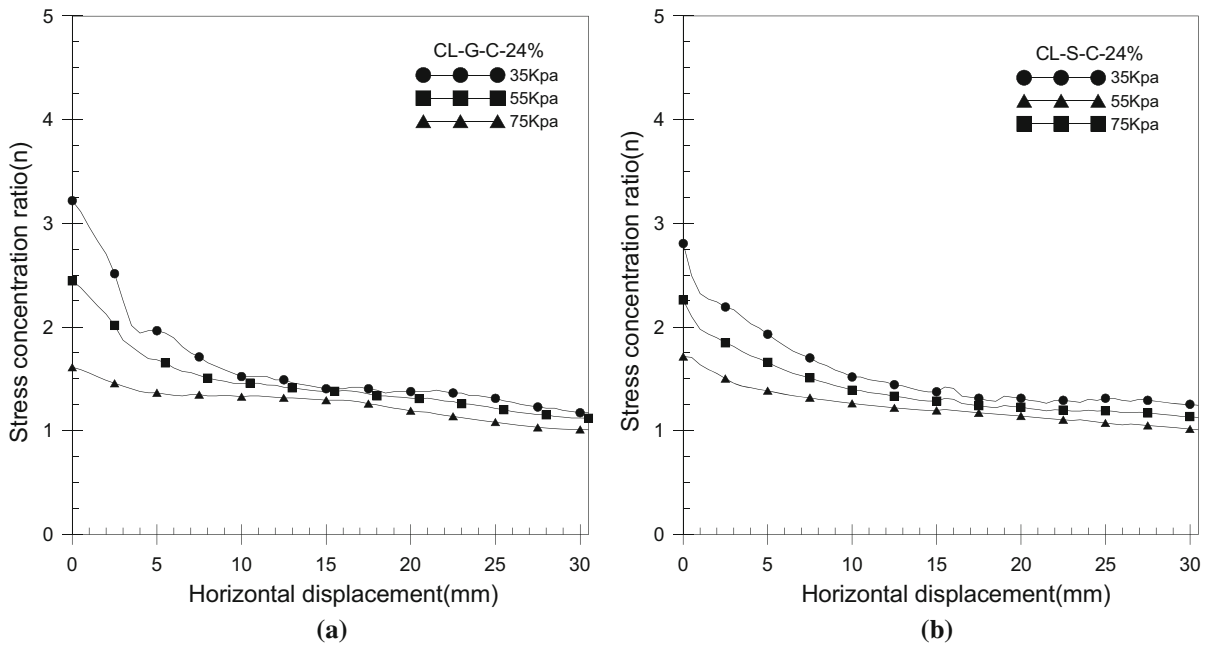


**Fig. 23** Stress concentration ratio for Ar = 24%: **a** CL-G-C, **b** CL-S-C

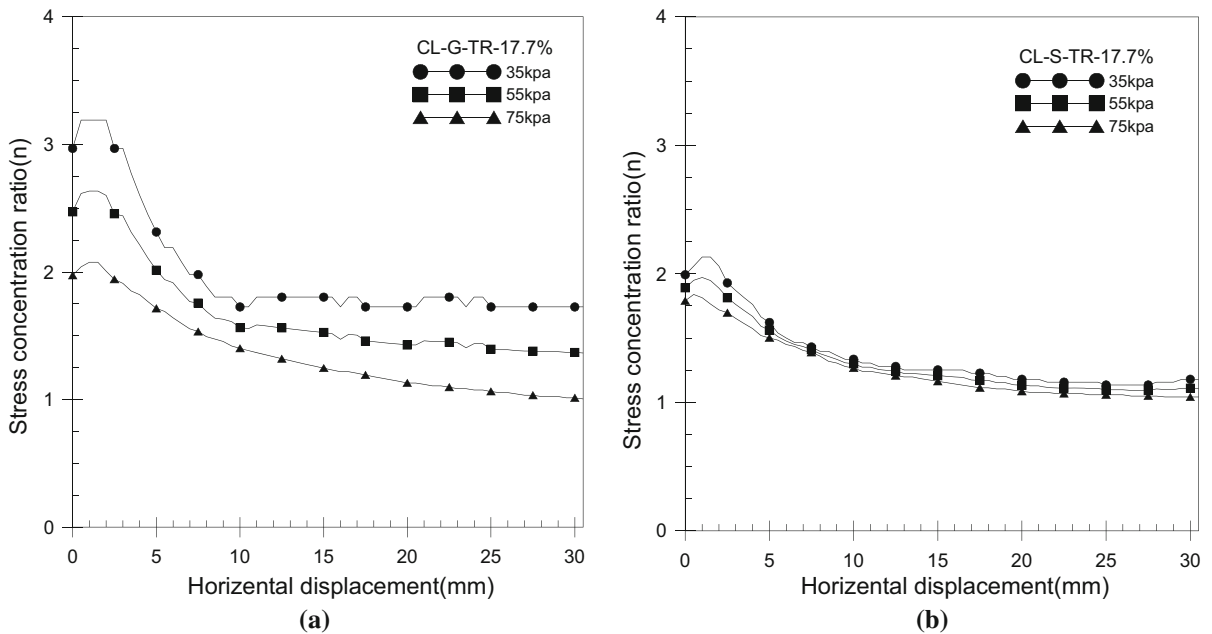


**Fig. 24** Stress concentration ratio for Ar = 17.7%: **a** CL-G-TR, **b** CL-S-TR

and equivalent shear strength parameters are assessed assuming that the value of stress concentration ratio is equal to 1. Priebe (1991,1995) included the effect of stress concentration ratio in assessing shear strength

parameters and proposed the following equations to predict  $\varphi_{ave}$ :

$$\varphi_{ave} = \arctg((\omega \cdot \tan \varphi_c) + (1 - \omega) \tan \varphi_s) \quad (7)$$

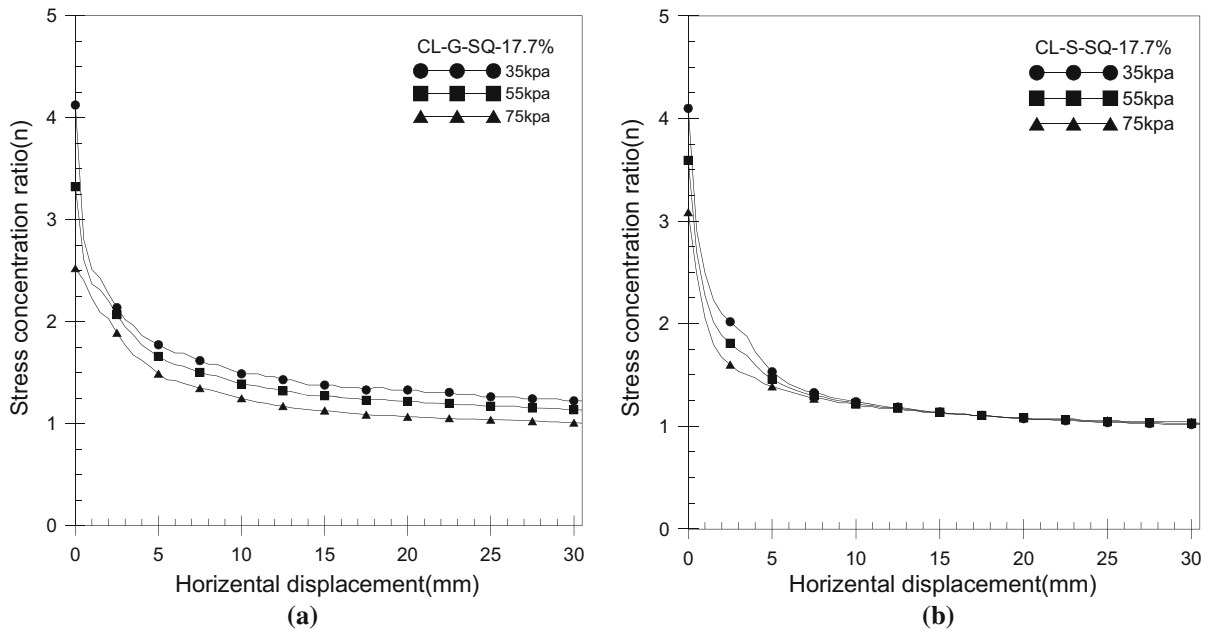


**Fig. 25** Stress concentration ratio for  $A_r = 17.7\%$ : **a** CL-G-SQ, **b** CL-S-SQ

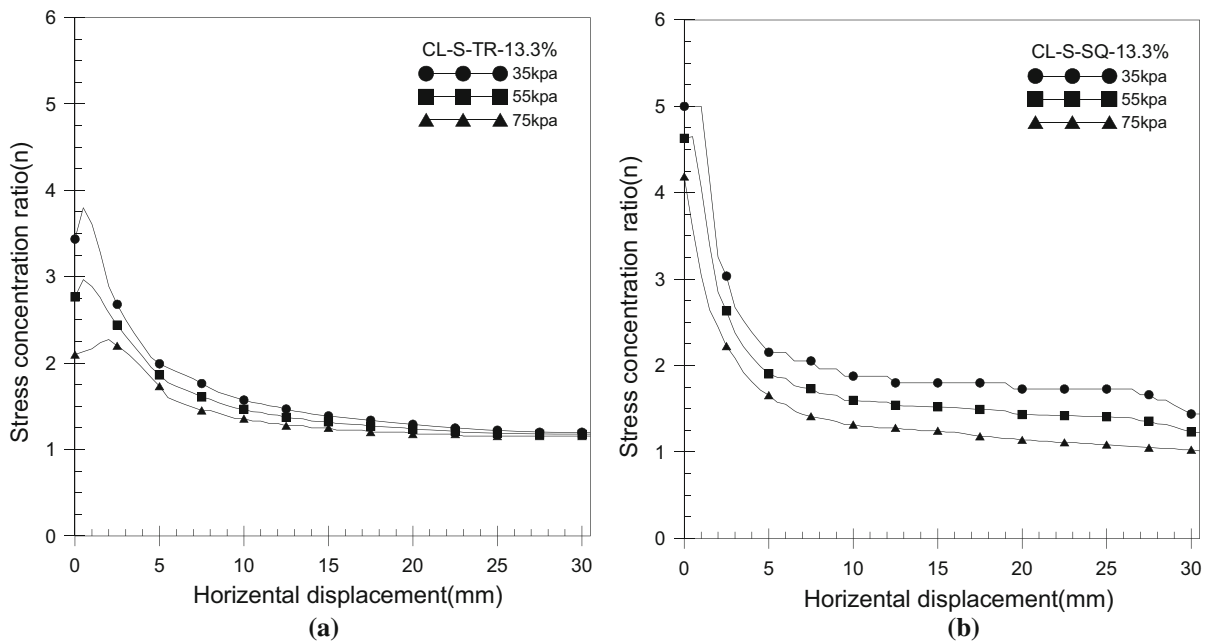


**Fig. 26** Stress concentration ratio for  $A_r = 13.3\%$ : **a** CL-S-TR, **b** CL-S-SQ

where  $\omega = \frac{A_r n}{1 + A_r(n-1)}$ ,  $A_r$  is area replacement ratio,  $n$  is stress concentration ratio,  $\phi_{ave}$  is equivalent friction angle,  $\phi_c$  is friction angle of stone column material, and  $\phi_s$  is friction angle of bed material.

Comparison between shear strength parameters obtained from experiments and those predicted using Eqs. (4)–(7) is presented in Table 8.

Figures 21, 22, 23, 24, 25 and 26 show that stress concentration ratio is linked to horizontal

**Table 8** Comparing the results of the experiments with the analytical relations

Vertical stress (kPa)	arrangement pattern	Area replacement ratio Ar (%)	Stress concentration ratio (n)		Internal friction angle from tests	The friction angle resulting from analytic relations with consideration (SCR) (Eq = 7) (°)			The friction angle resulting from analytic relations without consideration (SCR) (°)		
			Max	Min		n = 1	n = 2	SCR (n) value required in relation 7	Eq. (4) Eq. (5) Eq. (6)		
									Eq. (4)	Eq. (5)	Eq. (6)
35	CL-G-C	24	3.21	1.17	10	10	16	1	10	10	9
55			2.44	1.12							
75			1.61	1							
35	CL-G-C	17.7	3.71	1.12	8	8	13	1	8	8	7
55			2.85	1.07							
75			1.98	1.02							
35	CL-G-C	13.3	5	1.39	6	6	10	1	6	6	5
55			4	1.25							
75			3.64	1							
35	CL-G-SQ	17.7	4.12	1.22	10	8	13	1.5	8	8	7
55			3	1.13							
75			2.52	1							
35	CL-G-TR	17.7	3.19	1.72	9	8	13	1.2	8	8	7
55			2.63	1.36							
75			2	1							
35	CL-S-C	24	2.8	1.24	9	9	14	1	8	9	8
55			2.26	1.12							
75			2.26	1.09							
35	CL-S-C	17.7	3.72	1.23	6	7	11	1	7	6	6
55			2.98	1							
75			2.24	1							
35	CL-S-C	13.3	4.96	1.31	5	5	9	1	5	5	5
55			3.74	1.17							
75			2.89	1.035							
35	CL-S-SQ	17.7	4.09	1.03	9	7	11	1.6	7	6	6
55			3.6	1.03							
75			3.08	1							
35	CL-S-SQ	13.3	5	1.44	7	5	9	1.5	5	6	5
55			4.63	1.22							
75			4.18	1.02							
35	CL-S-TR	17.7	2.13	1.17	8	7	11	1.3	7	6	6
55			1.97	1.11							
75			1.81	1.04							
35	CL-S-TR	13.3	3.79	1.2	6	5	9	1.2	5	5	5
55			2.9	1.17							
75			2.27	1.15							

displacement level, and gets its highest value at the beginning of the experiment, and decreases with the increase of horizontal displacement. However, the substantial question is what value of ( $n$ ) should be used in calculations. In this study, after determining the internal friction angle in each experiment the stress concentration ratio was back-calculated using Eq. (7) through an inverse analysis. The obtained values were then compared with values of stress concentration ratio measured by load cells. Results showed that in calculating shear strength parameters the maximum value of ( $n$ ) should not be used. Instead, stress concentration ratio value approximately corresponding to the final horizontal displacement should be used. For single stone columns, shear strength parameter values obtained from experiments are equal to the values predicted by analytical relationships assuming a stress concentration ratio of 1. For square and triangular patterns the experimental results are equal to the shear strength values predicted by Eq. (7) at stress concentration ratios of 1.5 and 1.3, respectively.

## 12 Conclusions

In this study, the behavior of stone columns subjected to shear loading was experimentally investigated. The behavior of stone columns was evaluated by performing direct shear tests with different area replacement ratios (13.3, 17.7 and 24%), different stone column installation patterns (single, square and triangular), and different normal stresses (35, 55 and 75 kPa). The key findings of this study are as follows:

1. Shear strength increases with increase of area replacement ratios in all stone column installation patterns. In gravel columns, shear strength increase was in the range of 33–58% under normal stress of 35 kPa, 50–92% under normal stress of 55 kPa and 62–108% under normal stress of 75 kPa, for different stone column patterns. In sand columns, shear strength increase was in the range of 25–58% under normal stress of 35 kPa, 42–75% under normal stress of 55 kPa and 46–85% under normal stress of 75 kPa, for different stone column patterns. The rate of shear strength increase was noticeable for modified area ratios greater than 15%, and slight for modified area ratios below 15%.
2. For stone columns with the same area replacement ratios, the installation pattern has an effective role in defining the shear strength. Group stone columns mobilize higher shear strength compared to single stone columns. Among the installation patterns investigated in this study, stone columns with square arrangement experienced the highest increase in shear strength value while single stone columns experienced the lowest. The reason of this behavior is that the lateral surface of stone columns increases when the installation pattern is changed from single column to square pattern. As a result, lateral confining pressure on the soil between stone columns increases.
3. The slope increase of shear strength-horizontal displacement curves shows that the soil-stone column system has higher stiffness than soft clay layer, and this stiffness varies with area replacement ratios and installation pattern. The maximum stiffness values refer to square arrangement of stone columns and the minimum values refer to single stone columns.
4. The equivalent shear strength values obtained from experiments are higher than those predicted by analytical relationships. Accordingly, it is conservative to use analytical relationships to calculate shear strength parameters. It is worth explaining that these relationships assume that stress concentration ratio is equal to 1. Results from this study show that the exact value of stress concentration ratio should be calculated and used in the relationships.
5. Comparison between shear strength parameters obtained from experiments and those predicted by analytical relationships shows that in single stone columns, the value of stress concentration ratio should be 1, and in square and triangular patterns, this value should be 1.5 and 1.3, respectively, to achieve good agreement between experimental and analytical results.

## References

- Abusharar SW, Han J (2011) Two-dimensional deep-seated slope stability analysis of embankments over stone column-improved soft clay. *Eng Geol* 120:103–110

- Barksdale RD, Bachus RC (1983) Design and construction of stone column, vol 1. FHWA/RD
- Chen JF, Li LY, Xue JF, Feng SZ (2015) Failure mechanism of geosynthetic encased stone columns in soft soils under embankment. *Geotext Geomembr J* 43(5):424–431
- Christoulas ST, Giannaros CH, Tsiambaos G (1997) Stabilization of embankment foundations by using stone columns. *Geotech Geol Eng J* 15:247–258
- Cooper MR, Rose AN (1999) Stone column support for an embankment on deep alluvial soils. *ICE Proc Geotech Eng* 137(1):15–25
- Das AK, Deb K (2017) Modeling stone columns-supported embankment under axis-symmetric condition. *Geotech Geol Eng* 35(2):707–730
- Fattah MY, Shlash T, Al-Waily MJK (2010) Stress concentration ratio of model stone columns in soft clays. *Geotech Test J* 34(1):1–11
- Fattah MY, Al-Neami M, Al-Suhaily AS (2017) Estimation of bearing capacity of floating group of stone columns. *Eng Sci Technol J* 20(3):1166–1172
- Fox ZP (2011) Critical state, dilatancy and particle breakage of mine waste rock. Master's thesis, Colorado State University, Fort Collins, USA
- Ghazavi M, Nazari Afshar J (2013) Bearing capacity of geosynthetic encased stone columns. *Geotext Geomembr J* 28:26–36
- Gniel J, Bouazza A (2008) Improvement of soft soils using geogrid encased stone columns. *Geotext Geomembr* 27(3):167–175
- Greenwood DA (1970) Mechanical improvement of soils below ground surface. In: Proceedings of ground improvement conference. Institute of Civil Engineering, pp 9–29
- Hasan M, Samadhiya NK (2016) Experimental and numerical analysis of geosynthetic-reinforced floating granular piles in soft clays. *Geosynth Ground Eng J* 2(22):1–13
- IS: 15284 (Part 1) (2003) Indian standard code of practice for design and construction for ground improvement-guidelines. Indian Standards Institution, New Delhi
- McKelvey D, Sivakumar V, Bell A, Graham J (2004) Modelling vibrated stone columns in soft clay. *Proc Inst Civ Eng Geotech Eng* 157(GE3):137–149
- Miranda M, Da Costa A, Castro J, Sagaseta C (2017) Influence of geotextile encasement on the behaviour of stone columns: laboratory study. *Geotext Geomembr J* 45(1):14–22
- Mohapatra SR, Rajagopal K, Sharma J (2016) Direct shear tests on geosynthetic-encased granular columns. *Geotext Geomembr J* 44(3):396–405
- Murugesan S, Rajagopal K (2006) Geosynthetic-encased stone columns: numerical evaluation. *Geotext Geomembr J* 24(6):349–358
- Murugesan S, Rajagopal K (2008) Shear load tests on stone columns with and without geosynthetic encasement. *Geotech Test J* 32(1):GTJ101219
- Murugesan S, Rajagopal K (2010) Studies on the behavior of single and group of geosynthetic encased granular columns. *Geotech Geoenviron Eng J* 136(1):129–139
- Najjar S, Sadek S, Maakaroun T (2010) Effect of sand columns on the undrained load response of soft clay. *J Geotech Geoenviron Eng ASCE* 136(9):1263–1277
- Nayak NV (1983) Recent advances in ground improvements by stone column. In: Proceedings of Indian geotechnical conference, IGC-83, Madras, India, vol 1, pp 5–19
- Nazariafshar J, Mehrannia N, Kalantary F, Ganjian N (2017) Bearing capacity of group of stone columns with granular blankets. *Int J Civ Eng*. <https://doi.org/10.1007/s40999-017-0271-y>
- Ng KS, Tan SA (2015) Simplified homogenization method in stone column designs. *Soils Found* 55(1):154–165
- Priebe HJ (1991) Vibro replacement—design criteria and quality control, ASTM STP 1089—deep foundation improvements-design. construction and testing
- Priebe HJ (1995) The design of vibro replacement. *Ground Eng J* 28(12):31–37
- Ranjan G (1989) Ground treated with granular piles and its response under load. *Indian Geotech J* 19(1):1–86
- Sivakumar V, McKelvey D, Graham J, Hughes D (2004) Triaxial test on model sand columns in clay. *Can Geotech J* 41(2):299–312
- Stoeber JN (2012) Effects of maximum particle size and sample scaling on the mechanical behavior of mine waste rock; a critical state approach. Master's thesis, Colorado State University, Fort Collins, USA
- Vekli M, Aytakin M, Ikizler SB, Calik U (2012) Experimental and numerical investigation of slope stabilization by stone columns. *Nat Hazards J* 64(1):789–820
- Yoo C (2010) Performance of geosynthetic-encased stone columns in embankment construction: numerical investigation. *Geotech Geoenviron Eng J* 136(8):1148–1160
- Yu Y, Bathurst RJ, Damians IP (2016) Modified unit cell approach for modelling geosynthetic-reinforced column-supported embankments. *Geotext Geomembr J* 44(3):332–343
- Zahmatkesh AM, Choobbasti AJ (2010) Investigation of bearing capacity and settlement of strip footing on clay reinforced with stone columns. *Aust J Basic Appl Sci* 4(8):3658–3668
- Zhang Z, Han J, Ye G (2014) Numerical investigation on factors for deep-seated slope stability of stone column-supported embankments over soft clay. *Eng Geol J* 168:104–113